

FIG. 3. Oscilloscope traces of pump pulse and spin-flip output pulse. Both were taken with the same amplifier gain setting.

the relative spin-flip output power as a function of the input pump power at a magnetic field of 78 kG. The strong saturation of the spin-flip output at the highest pump intensities is attributed to spin saturation. At the highest pump intensities, the spin-flip output pulse became flat-topped and did not change its shape or intensity as the pump intensity was increased further. This is shown in the oscilloscope trace of Fig. 3. The upper trace is the HF pump pulse and the lower trace is the spin-flip output pulse, both taken with the same amplifier gain setting. For pump intensities below that where spin saturation occurred, pump depletion was observed, indicating an efficient conversion of pump radiation to Stokes radiation. For input power levels below about 100 W, conversion efficiencies in excess of 20% were observed. The input pump intensity was varied by inserting flat glass attenuators in the beam in order not to alter the laser mode structure. The stimulated spin-flip output was determined to be collinear with the pump by

scanning the output from the exit face of the crystal.

No stimulated emission was detected below a magnetic field of 59 kG for these samples although the calculated quantum limit at 0 K was about 41 kG. Substantial resonant enhancement of the Raman cross section is obtained by operating close to the band gap. For the  $3385.34\text{-cm}^{-1}$  HF laser pump line this is estimated to be about  $10^3$ . A substantial reduction of the resonant enhancement factor would result in higher thresholds for pumping with DF laser lines.

The tuning rate for the first Stokes component was nearly linear in the range 59–85 kG and was 17.7 GHz/kG. A least-squares fit of the data to a three-band non-parabolic model was made and a zero-field  $g$  factor of  $15.28 \pm 0.15$  was obtained using an energy gap of 0.41 eV, a spin-orbit splitting of 0.44 eV, and an effective mass of  $0.024m_0$ . This value for the  $g$  factor agrees well with the  $g$  factor of about 15 obtained from the magneto-optical absorption measurements of Pidgeon *et al.*<sup>4</sup> and from the spontaneous spin-flip Raman scattering by Patel and Slusher.<sup>5</sup>

The technical assistance of R. Belanger, W.E. Barch, D.J. Wells, and W.E. DeFeo is gratefully acknowledged along with helpful discussions with S.R.J. Brueck and H.J. Zeiger.

\*Work sponsored by the Department of the Air Force.

<sup>1</sup>C.K.N. Patel and E.D. Shaw, *Phys. Rev. Lett.* **24**, 451 (1970); *Phys. Rev. B* **3**, 1279 (1971).

<sup>2</sup>A. Mooradian, S.R.J. Brueck, and F.A. Blum, *Appl. Phys. Lett.* **17**, 481 (1970); S.R.J. Brueck, A. Mooradian, and F.A. Blum, *Phys. Rev. B* **7**, 5253 (1973).

<sup>3</sup>J.F. Scott, T.C. Damen, and P.A. Fleury, *Phys. Rev. B* **6**, 3856 (1972).

<sup>4</sup>C.R. Pidgeon, D.L. Mitchell and R.N. Brown, *Phys. Rev.* **154**, 737 (1967).

<sup>5</sup>C.K.N. Patel and R.E. Slusher, *Phys. Rev.* **167**, 413 (1968).

## Identification of the dominant diffusing species in silicide formation

W. K. Chu, H. Kräutle, J. W. Mayer, H. Müller, and M.-A. Nicolet\*

California Institute of Technology, Pasadena, California 91109

K. N. Tu†

IBM Thomas J. Watson Research Center, Yorktown Heights, New York 10598

(Received 24 May 1974)

Implanted noble gas atoms of Xe have been used as diffusion markers in the growth study of three silicides:  $\text{Ni}_2\text{Si}$ ,  $\text{VSi}_2$ , and  $\text{TiSi}_2$ . Backscattering of MeV He has been used to determine the displacement of the markers. We found that while Si atoms predominate the diffusion in  $\text{VSi}_2$  and  $\text{TiSi}_2$ , Ni atoms are the faster moving species in  $\text{Ni}_2\text{Si}$ .

The subject of silicide formation by thin-film contact reaction has recently attracted wide attention.<sup>1-5</sup> This is because of the technical importance of silicides used as contact layers in silicon devices and also because of

the advances made in analysis by MeV ion backscattering and glancing angle x-ray diffraction.<sup>1</sup> While a large number of silicides have been studied, there are still many aspects of silicide formation that are far from

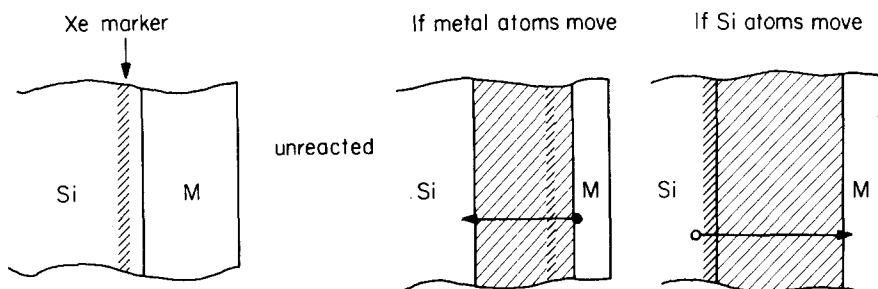


FIG. 1. Schematic diagrams of implanted marker and marker displacements during silicide formation. The marker will shift toward the surface if metal atoms are the dominant diffusion species and will shift deeper into the sample if the dominant diffusing species is silicon.

understood. For example, the identification of the dominant diffusing species during the formation of a silicide is not known and yet is crucial to the understanding of how a silicide grows. Information about diffusing species cannot be obtained by growth measurements but can be determined by a marker experiment.<sup>6</sup> We note that there are earlier efforts devoted to obtaining such information by profiling the Ar impurity as in the case of HfSi<sup>7</sup> and by the simultaneous growth of two silicides as in the case of Pt<sub>2</sub>Si and PtSi.<sup>8</sup> These approaches are, however, limited to special cases and do not show the potential of general applications. In this letter, we report the use of implanted noble gas atoms as markers and the use of MeV He ion backscattering to determine the displacement of the markers.<sup>9</sup> The implanted marker concept appears to have a general application to thin-film reactions.

The combination of implanted noble gas markers and backscattering techniques has been used by Brown and Mackintosh in the study of the anodic oxidation of aluminum.<sup>10</sup> From the displacement of the implanted markers relative to the sample surface during oxidation, they determined the amount of transport of both oxygen and aluminum. The application of this marker concept to silicide formation is shown schematically in Fig. 1. Samples of silicon are implanted with Xe, for example, and then covered with a thin ( $\approx 1000 \text{ \AA}$ ) layer of metal. When the sample is heated to form a silicide layer, the marker will shift toward the surface if metal atoms are the dominant diffusing species. If the dominant diffusing species is silicon, the marker will be displaced deeper into the sample. Therefore, from the displacement of the marker relative to the surface, one can determine the identity of the diffusing species during silicide growth.

Because MeV He backscattering techniques are used to establish a depth scale, the marker and metal combination must be selected so that the positions of the marker can be clearly identified in the energy spectra of backscattered particles. In the present investigation we utilized Xe and the medium-mass metals Ni, V, and Ti. Reactions of these metals with silicon to form silicides have been reported.<sup>2,5,11</sup> Silicon samples were implanted with 100-keV Xe to a dose of  $1-2 \times 10^{15} \text{ Xe/cm}^2$ . The thickness of the deposited metal layer was chosen such that signals from the Xe marker could be resolved without interference. In some cases Xe was implanted into Ni and V layers for an independent check of the method.

The energy spectrum for 2-MeV <sup>4</sup>He ions scattered from a silicon sample with 1300  $\text{\AA}$  of Ni is shown by

open circles in Fig. 2(a). The implanted Xe appears at 1.6 MeV, an energy which is approximately 160 keV below the energy corresponding to Xe at the sample surface. After heat treatment at 325  $^{\circ}\text{C}$  for 20 min, the silicide Ni<sub>2</sub>Si is formed and the Xe marker is displaced toward higher energies, i.e., toward the sample surface. The broadening of the Xe peak after incorporation into the silicide is due primarily to the increased stopping cross section of the MeV He ions in Ni<sub>2</sub>Si (as compared to that of Si) rather than a diffusional spreading of the Xe distribution.

The amount of displacement of the Xe marker is related to the silicide thickness. The Xe position below the surface versus silicide thickness is shown in Fig. 2(b) for different samples and heat treatments. The two dashed lines correspond to the calculated Xe positions under the assumption that either Si or Ni is the diffusing species. The agreement of the data points with the lower dashed line indicates that the mass transport involved in the formation of Ni<sub>2</sub>Si is predominantly the metal species, Ni.

For V and Ti silicides, the opposite case is found, i.e., the Xe marker is displaced toward greater depths indicating that Si transport is dominant. This is shown in Fig. 3(a) for V deposited on Si and then reacted at 500  $^{\circ}\text{C}$ . In Fig. 3(b), the Xe marker position versus total layer thickness is shown for several samples of VSi<sub>2</sub> and TiSi<sub>2</sub>. The dashed line which corresponds to the case in which only Si is the diffusing species also corresponds to Xe located at the Si/silicide interface.

For samples with Xe implanted into the vanadium layer rather than Si, the Xe also was displaced to greater depths. However, the position of Xe was not shifted during heat treatment until the advancing silicide phase reached the marker. At this point the marker was incorporated in VSi<sub>2</sub> and was shifted to lower energies. This again is consistent with the identity of Si as the diffusing species.

The results shown in Figs. 2 and 3 indicate that during the formation of the three silicides, the mass transport is almost completely dominated by the diffusion of one of the species, either Si or metal. The case of Ni<sub>2</sub>Si is the first silicide reported in which the metal is the diffusing species. We note also that of the three silicides discussed in this work, Ni<sub>2</sub>Si has the lowest temperature of formation (200–350  $^{\circ}\text{C}$ ). If the diffusion occurs by exchange with vacancies, the structure of Ni<sub>2</sub>Si favors diffusion of Ni rather than that of Si, since Ni has both Ni and Si as first nearest neighbors whereas

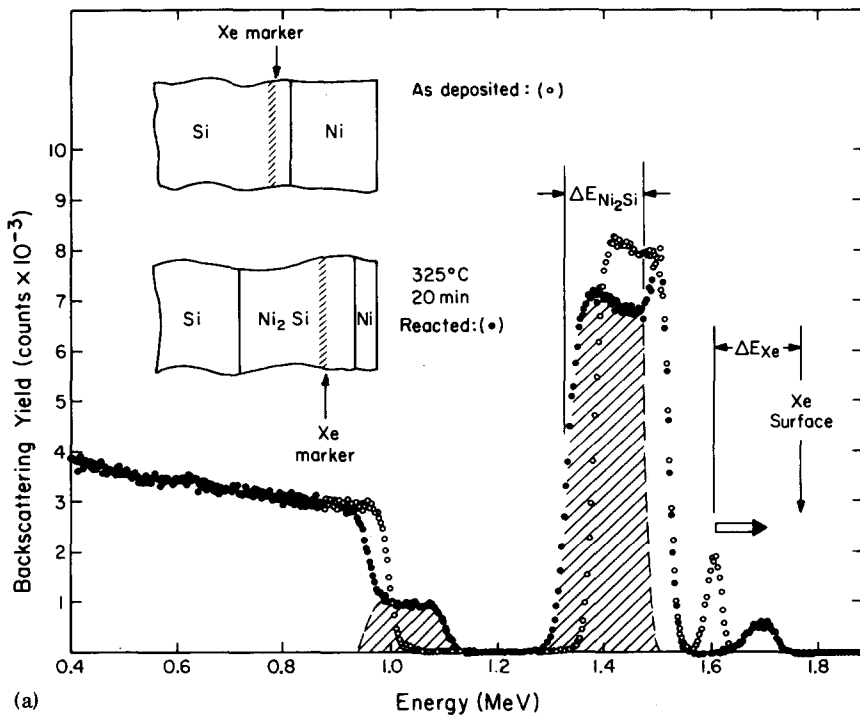
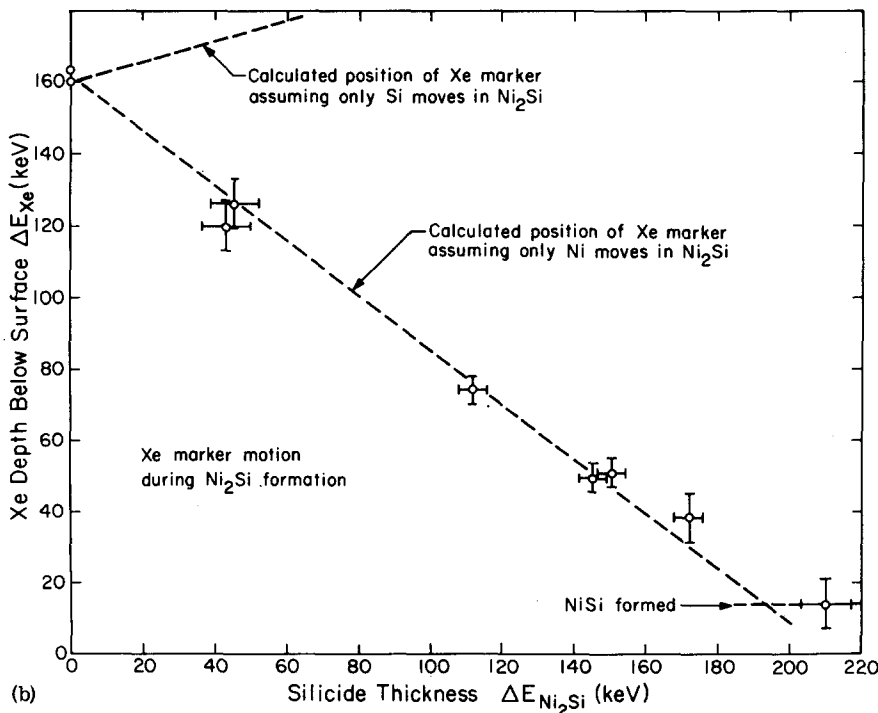


FIG. 2. (a) Energy spectra for 2-MeV  $^4\text{He}^+$  ions scattered from a silicon sample covered with 1300 Å of Ni before and after the formation of  $\text{Ni}_2\text{Si}$  (shaded area). The displacement toward the surface of the implanted Xe markers can be seen at the high-energy side. (b) The amount of displacement of the Xe marker vs the thickness of  $\text{Ni}_2\text{Si}$  silicide. The two dashed lines correspond to the energy shift of the Xe under the assumption that either Si or Ni is the diffusing species.



the Si nearest neighbors are Ni. This same argument may also apply to other metal-rich silicides.

When the marker is introduced into the silicon by implantation, radiation damage occurs which could influence silicide formation. To investigate this possibility, a few of the Xe-implanted Si samples (for each system studied) were annealed at 700 °C before the V, Ti, or Ni layers were deposited. The displacement of the marker during silicide formation was the same for annealed and nonannealed samples. Furthermore, with the formation of silicide layers of about 1000-Å thickness, the consumed amount of Si extends well beyond the damaged layer. We conclude that damage effects

did not change the role of the marker in the present experiments.

The implanted Xe has a projected range of about 200 Å in Si and corresponds to a concentration of 1–2 at. % for implanted doses of  $2 \times 10^{15}/\text{cm}^2$ . During heat treatment the implanted Xe may remain dispersed as atomic species or may coalesce into bubbles. If implanted Xe coalesces into bubbles, solubility effects will not be important. In this case the Xe bubbles will act as inert markers. However, in the other case, the atomic species might be rejected from the silicide due to solubility effects when the silicide front reaches the Xe. Hence the marker would remain trapped at the inter-

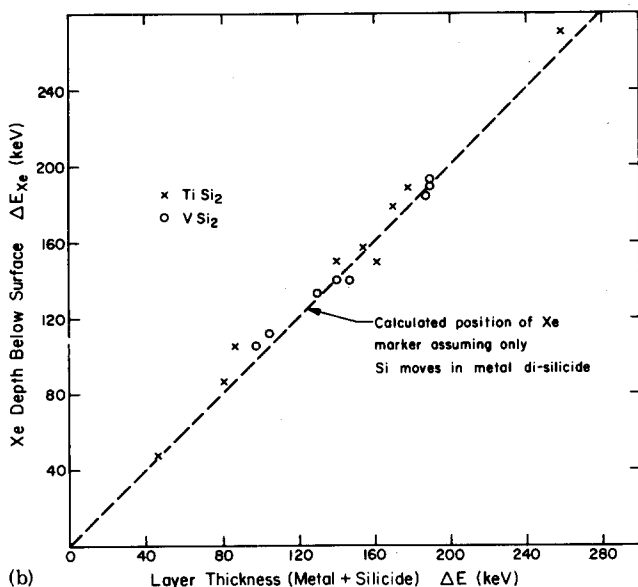
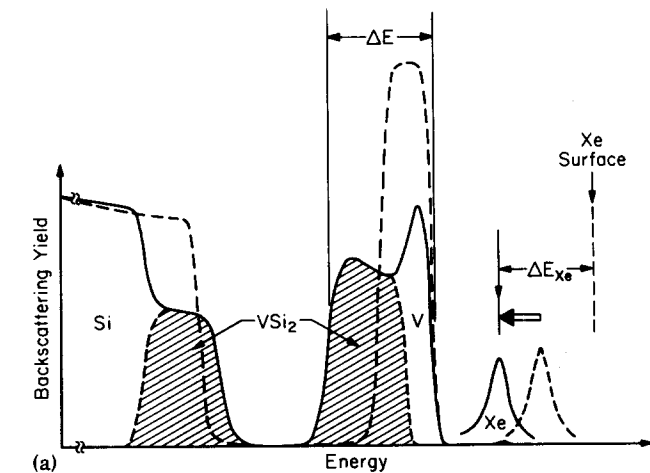


FIG. 3. (a) The sketched energy spectra of backscattered ions from a V/Si sample before and after the  $VSi_2$  formation. The displacement into the Si of the implanted Xe markers can be seen at the high-energy side. (b) The amount of displacement of the Xe marker vs the thickness of the metal plus silicide layer. The dashed line corresponds to the energy shift of the Xe under the assumption that Si is the diffusing species.

face. This solubility effect would lead to a marker displacement that could be interpreted as evidence for Si migration. The interpretation can be tested (as in the

present work for vanadium) by implanting Xe into the metal and noting the displacement of the Xe. In both cases (implantation into Si or metal) the marker should shift in the same direction if solubility effects are not effective. Alternatively, one could preform a silicide layer and then implant into the silicide before deposition of the metal layer. It should be noted that in the anodic oxidation of aluminum, it has also been found that some species are swept into the metal by the advancing oxide front.<sup>10</sup>

Marker displacement cannot distinguish between mass transport by grain boundary diffusion and lattice diffusion. However, the marker will displace as long as the diffusion mechanism is nonconservative.

In summary, we have shown the implanted noble gas atoms can be used as diffusion markers in silicide formation. While Si atoms are found to dominate the diffusion in  $VSi_2$  and  $TiSi_2$ , Ni atoms are the faster moving species in  $Ni_3Si$ . Ni is the first case in which the metal atom is found to diffuse faster than the Si atom.

\*Work supported in part by Office of Naval Research (L. Cooper).

†Work supported in part by ARPA Contract administered by AFCRL.

<sup>1</sup>J.W. Mayer and K.N. Tu, *J. Vac. Sci. Technol.* 11, 86 (1974).

<sup>2</sup>R.W. Bower and J.W. Mayer, *Appl. Phys. Lett.* 20, 359 (1972).

<sup>3</sup>J.F. Ziegler, J.W. Mayer, C.J. Kircher, and K.N. Tu, *J. Appl. Phys.* 44, 3851 (1973).

<sup>4</sup>G.A. Huchins and A. Shepala, *Thin Solid Films* 18, 343 (1973).

<sup>5</sup>K.N. Tu, J.F. Ziegler, and C.J. Kircher, *Appl. Phys. Lett.* 23, 493 (1973).

<sup>6</sup>E.O. Kirkendall, *Trans AIME* 147, 104 (1942).

<sup>7</sup>C.J. Kircher, J.W. Mayer, K.N. Tu, and J.F. Ziegler, *Appl. Phys. Lett.* 22, 81 (1973).

<sup>8</sup>J.M. Poate and T.C. Tisone, *Appl. Phys. Lett.* 24, 391 (1974).

<sup>9</sup>W.K. Chu, H. Krautle, J.W. Mayer, M.-A. Nicolet, and K.N. Tu, *Bull. Am. Phys. Soc.* 19, 273 (1974).

<sup>10</sup>F. Brown and W.D. Mackintosh, *J. Electrochem. Soc.* 120, 1096 (1973).

<sup>11</sup>K.N. Tu, E.I. Alessandrini, W.K. Chu, H. Krautle, and J.W. Mayer, *Jpn J. Appl. Phys.* (to be published).